



CLASSIFICATION OF HYPERSPECTRAL DATA

B23APV01

PALLE PRANAY REDDY
Z RAM GOPAL
V GOWTHAM

MENTORED BY: Dr. ARUN PV

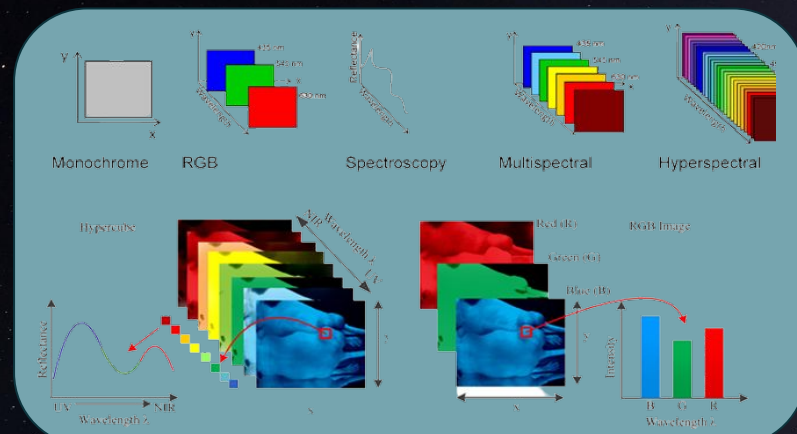


TABLE OF CONTENTS

01

Introduction

02

Motivation

03

Problem
Statement

04

Data info

05

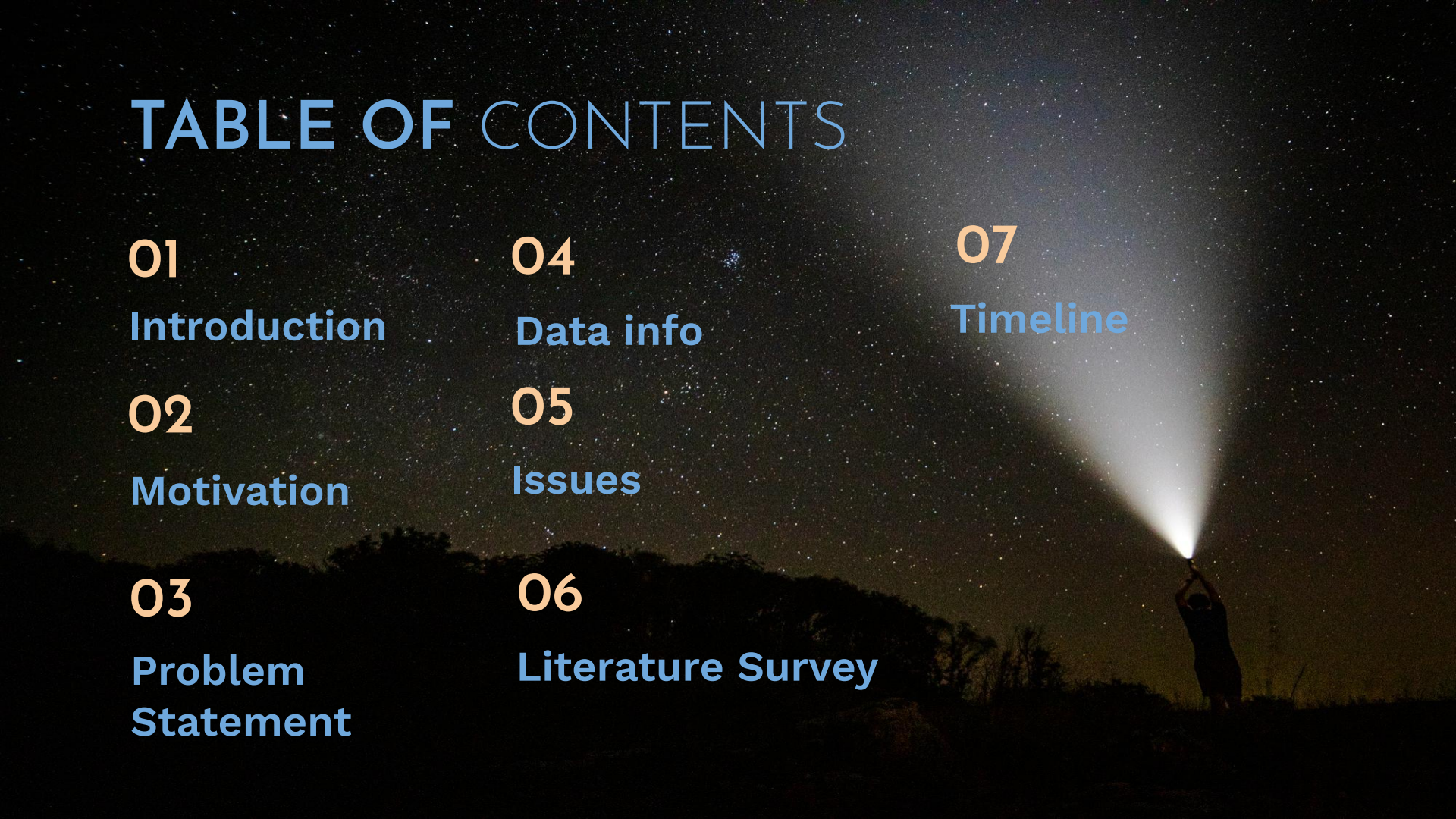
Issues

06

Literature Survey

07

Timeline



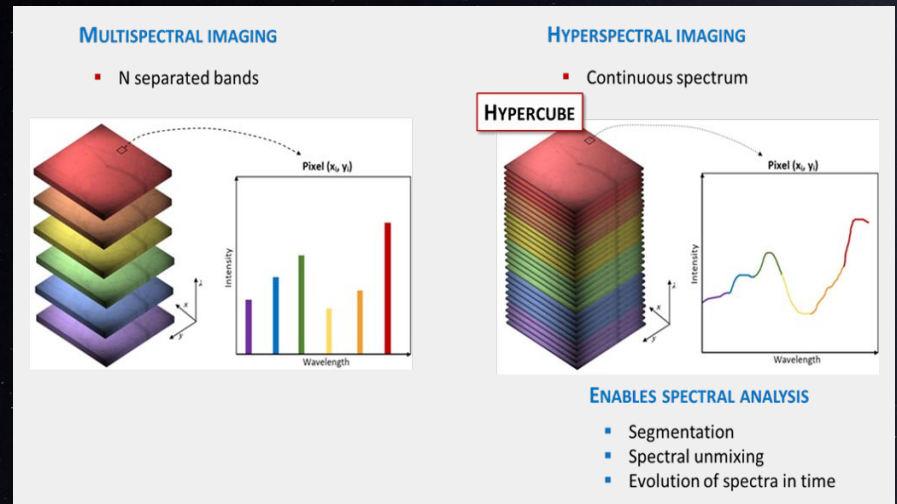
01

INTRODUCTION

INTRODUCTION

What is HyperSpectral Data ?

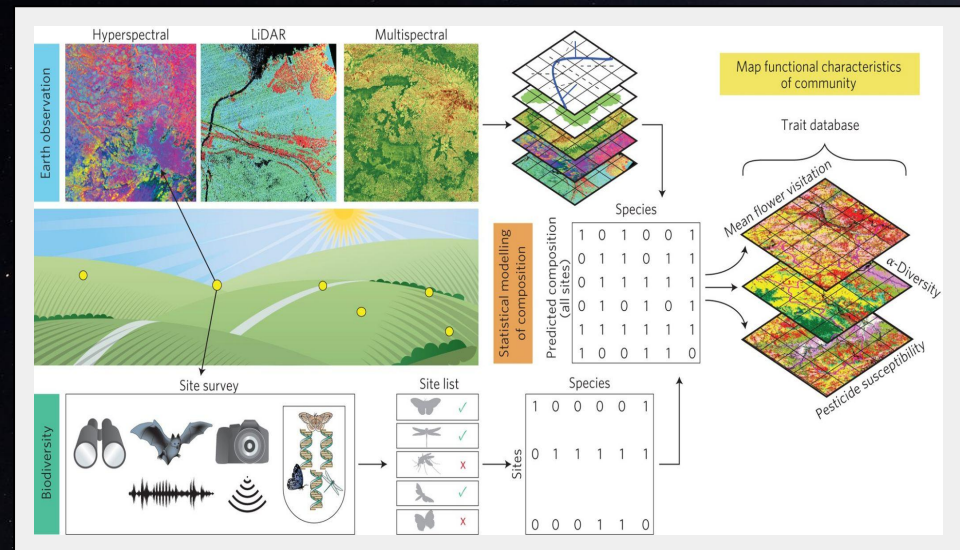
- Unlike traditional RGB images, which only capture three bands of color (red, green, and blue), hyperspectral data can capture hundreds or even thousands of narrow and contiguous bands that cover a much wider range of the electromagnetic spectrum.
- Hyperspectral Imaging collects hundreds of channels at different wavelengths for the same spatial area.
- Each channel covers a certain range of wavelength of light reflected by the surface that is imaged.



INTRODUCTION

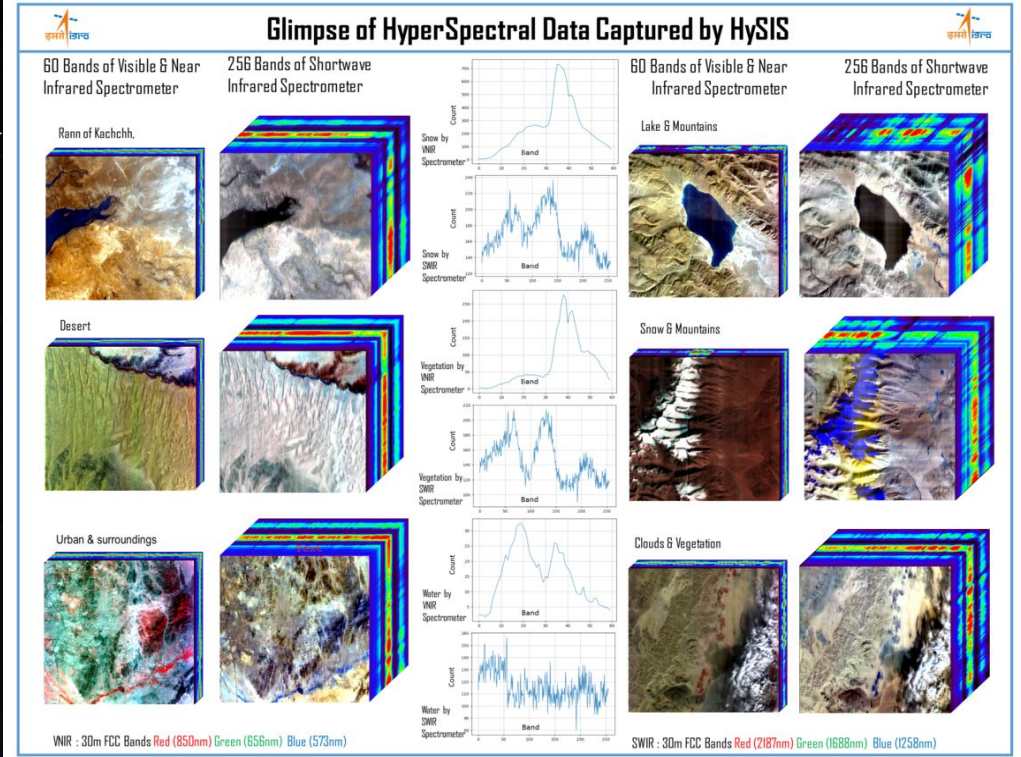
HyperSpectral Data ?

- The collected data form a so-called hyperspectral cube, in which two dimensions represent the spatial extent of the scene and the third its spectral content.
- HSI has variety of applications, including remote sensing, environmental monitoring, mineral exploration, to map minerals in rocks and medical imaging in the field of computer vision



02

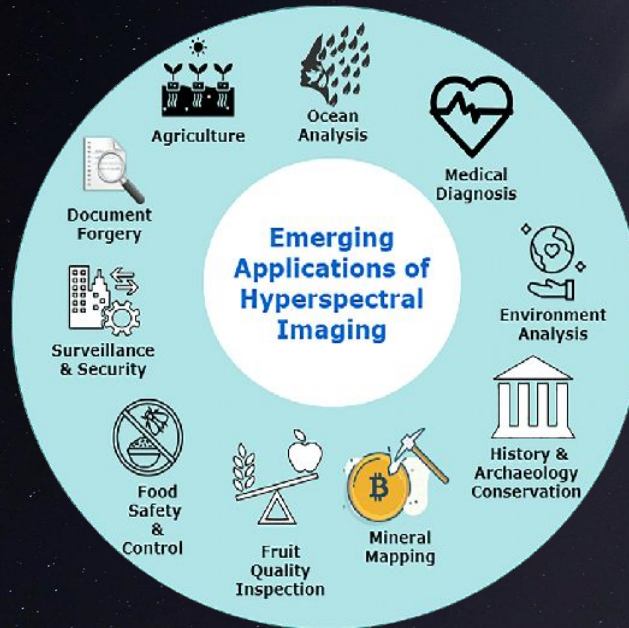
MOTIVATION



MOTIVATION

Why HyperSpectral Data ?

- Hyperspectral data provides a level of detail and accuracy that is not available with other types of remote sensing data. The ability to analyze materials in multiple bands across the electromagnetic spectrum allows for more precise identification of materials and objects.
- The detailed information captured in hyperspectral data can lead to new insights, such as identifying new mineral deposits.
- Hyperspectral imaging is employed in different fields such as astronomy, agriculture, molecular biology, biomedical imaging, mineralogy, geology, physics, cultural heritage, food processing, environment and surveillance



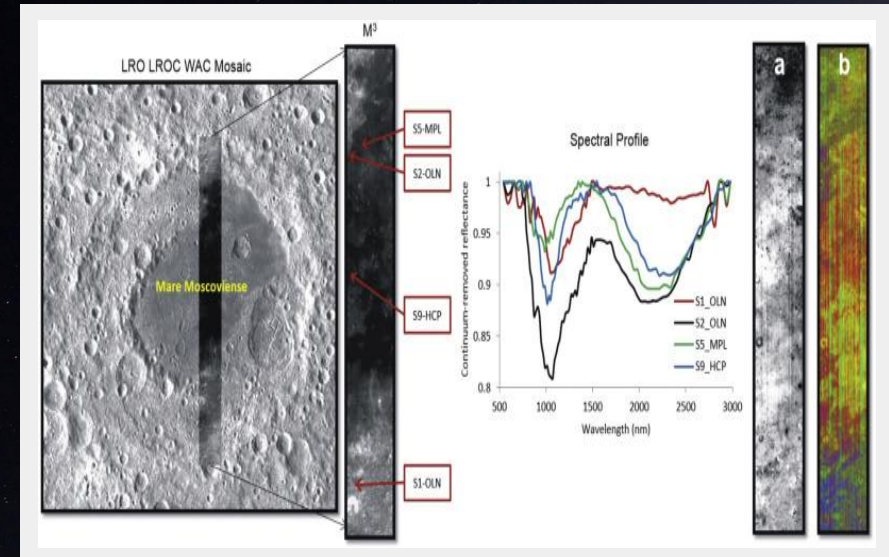
03

PROBLEM STATEMENT

PROBLEM STATEMENT

Mapping of Lunar Surface using Hyperspectral Image Classification

The hyperspectral data offers a platform for differentiating between minerals on the lunar surface, improving our comprehension of the composition of the moon's surface.



04

DATA INFORMATION

DATA INFORMATION

We are working on *Chandrayaan 2 IIRS data*.

Here's a brief information about IIRS:

Chandrayaan 2 Imaging Infrared Spectrometer
(IIRS)

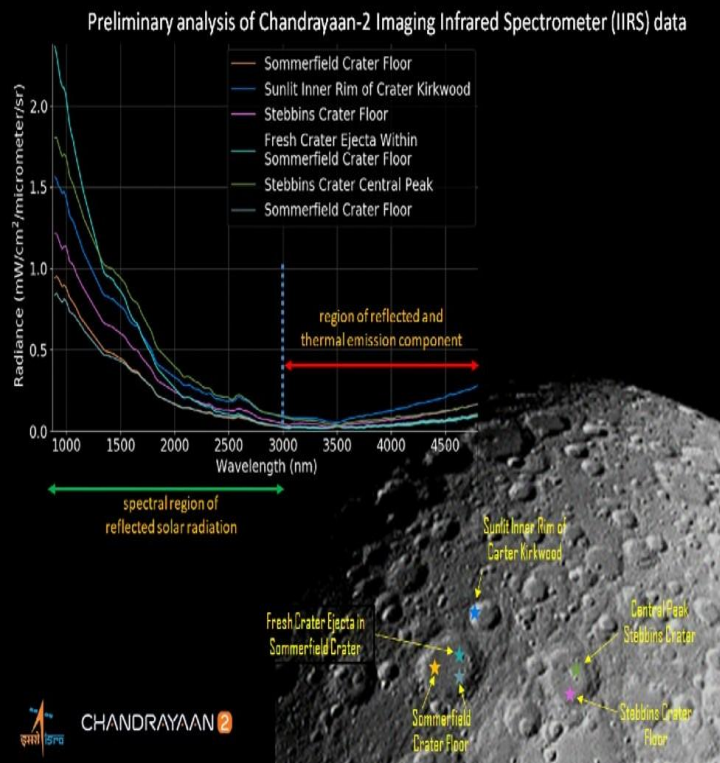
IIRS is designed to measure light from the lunar surface in narrow spectral channels (bands). It has the ability to split and disperse reflected sunlight (and its emitted component) into these spectral bands.

From the reflected solar spectrum, scientists will look for signatures, including of minerals. This will help map the lunar surface composition, which in turn will help us understand the Moon's origin and evolution in a geologic context.



DATA INFORMATION

Information about the data: Chandrayaan 2 IIRS Data



- 01 Altitude - 100km
- 02 Spatial Resolution - 80m
- 03 Spectral Resolution - 20 to 25 nm
- 04 Spectral Range - 0.8 to 5 μm
- 05 No. of Bands - Around 250

05

ISSUES

ISSUES

Coarse spectral and spatial data

The smallest area resolved by the sensor is relatively large which means the details captured by the sensor are very less.

Noisy nature of data

Data is subjected to noise due to atmospheric effects of lunar surface and instrumental (sensor) noises.

Limited samples

Lack of enough samples cause model overfitting during training which significantly affects the model's performance.

Spatial and spectral context

Examining and labelling each pixel individually will not yield good results. The local spatio-spectral relationships of neighboring individual pixel vectors must also be studied.

06

LITERATURE SURVEY

LITERATURE SURVEY - I

Title: HybridSN: Exploring 3D-2D CNN Feature Hierarchy for Hyperspectral Image Classification

Author(s): Swalpa Kumar Roy, Student Member, IEEE, Gopal Krishna, Shiv Ram Dubey, Member, IEEE, and Bidyut B. Chaudhuri, Life Fellow, IEEE

Overview of HybridSN

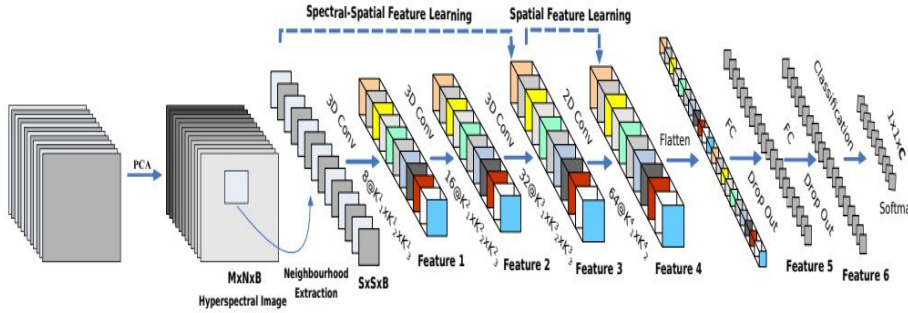
- HybridSN is a study on hyperspectral image classification that explores the use of a hierarchical feature extraction approach combining 3D-CNN and 2D-CNN.
- The approach consists of two main components: a 3D-CNN that extracts spectral features from the hyperspectral data, and a 2D-CNN that extracts spatial features from the output of the 3D-CNN.
- The proposed HybridSN model achieved improved classification performance compared to existing models on several benchmark hyperspectral datasets.

LITERATURE SURVEY - I

Data Set(s)

- Indian Pines Dataset
- University of Pavia
- Salinas Scene Dataset

The flow diagram of HybridSN model



Result

TABLE III: The training time in minutes (m) and test time in seconds (s) over IP, UP, and SA datasets using 2D-CNN, 3D-CNN and *HybridSN* architectures.

Data	2D CNN		3D CNN		HybridSN	
	Train(m)	Test(s)	Train(m)	Test(s)	Train(m)	Test(s)
IP	1.9	1.1	15.2	4.3	14.1	4.8
UP	1.8	1.3	58.0	10.6	20.3	6.6
SA	2.2	2.0	74	15.2	25.5	9.0

TABLE IV: The impact of spatial window size over the performance of *HybridSN*.

Window	IP(%)	UP(%)	SA(%)	Window	IP(%)	UP(%)	SA(%)
19×19	99.74	99.98	99.99	23×23	99.31	99.96	99.71
21×21	99.73	99.90	99.69	25×25	99.75	99.98	100

TABLE V: The classification accuracies (in percentages) using proposed and state-of-the-art methods on less amount of training data, i.e., 10% only.

Methods	Indian Pines			Univ. of Pavia			Salinas Scene		
	OA	Kappa	AA	OA	Kappa	AA	OA	Kappa	AA
2D-CNN	80.27	78.26	68.32	96.63	95.53	94.84	96.34	95.93	94.36
3D-CNN	82.62	79.25	76.51	96.34	94.90	97.03	85.00	83.20	89.63
M3D-CNN	81.39	81.20	75.22	95.95	93.40	97.52	94.20	93.61	96.66
SSRN	98.45	98.23	86.19	99.62	99.50	99.49	99.64	99.60	99.76
HybridSN	98.39	98.16	98.01	99.72	99.64	99.20	99.98	99.98	99.98

LITERATURE SURVEY - II

Title: Graph Convolutional Networks for Hyperspectral Image Classification

Author(s): Danfeng Hong , Member, IEEE, Lianru Gao , Senior Member, IEEE, Jing Yao , Bing Zhang , Fellow, IEEE, Antonio Plaza , Fellow, IEEE, and Jocelyn Chanussot , Fellow, IEEE

Overview of GCN in Feature Space for Image

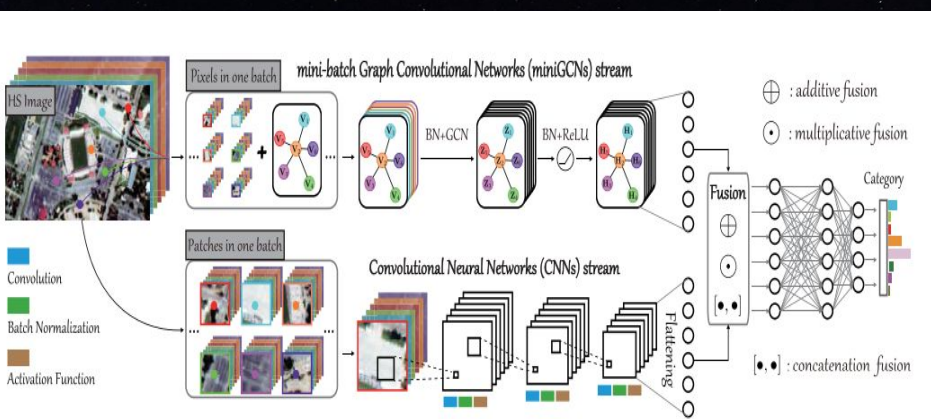
- Graph Convolutional Networks (GCNs) capable of taking advantage of both spatial and spectral information. Hence they can be used for Hyperspectral Image Classification
- Since GCNs have drawbacks like high computational cost, allowance of only full-batch network learning etc., the authors proposed miniGCNs which follows mini-batch learning and overcomes the above mentioned drawbacks.
- The experimental results, conducted on three widely used HS data sets, demonstrate the effectiveness and superiority of the proposed miniGCNs compared to the traditional GCNs.

LITERATURE SURVEY - II

Data Set(s)

- Indian Pines
- Pavia University
- Houston2013

The flow diagram of GCN model



Result

TABLE V
QUANTITATIVE COMPARISON OF DIFFERENT ALGORITHMS IN TERMS OF OA, AA, AND κ ON THE INDIAN PINES DATA SET. THE BEST ONE IS SHOWN IN BOLD

Class No.	KNN	RF	SVM	1-D CNN	2-D CNN	3-D CNN	GCN	miniGCN	FuNet-A	FuNet-M	FuNet-C
1	45.45	57.80	67.34	47.83	65.90	66.26	65.97	72.54	68.64	69.51	68.50
2	46.94	56.51	67.86	42.35	76.66	71.94	72.70	55.99	80.99	82.40	79.59
3	77.72	80.98	93.48	60.87	92.39	97.28	87.50	92.93	95.11	94.57	99.46
4	84.56	85.68	94.63	89.49	93.96	95.06	93.74	92.62	96.64	96.42	95.08
5	80.06	79.34	88.52	92.40	87.23	88.09	91.39	94.98	95.41	96.99	95.70
6	97.49	95.44	94.76	97.04	97.27	98.18	97.49	98.63	99.32	99.54	99.54
7	64.81	77.56	73.86	59.69	77.23	75.38	75.38	64.71	72.98	76.80	75.93
8	48.68	58.85	52.07	65.38	57.03	56.29	51.70	68.78	70.31	58.97	68.90
9	44.33	62.23	72.70	93.44	72.87	78.01	62.77	69.33	74.82	74.82	71.63
10	96.30	95.06	98.77	99.38	100.00	100.00	96.91	98.77	99.38	99.38	99.38
11	74.28	88.75	86.17	84.00	92.85	90.59	86.25	87.78	85.93	79.50	89.55
12	15.45	54.24	71.82	86.06	88.18	90.30	66.97	50.00	93.03	91.21	91.52
13	91.11	97.78	95.56	91.11	100.00	100.00	95.56	100.00	100.00	100.00	100.00
14	33.33	56.41	82.05	84.62	84.62	74.36	71.79	48.72	79.49	82.05	94.87
15	81.82	81.82	90.91	100.00	100.00	100.00	81.82	72.73	100.00	100.00	100.00
16	40.00	100.00	100.00	80.00	100.00	100.00	80.00	100.00	100.00	100.00	100.00
OA (%)	59.17	69.80	72.36	70.43	75.89	75.48	71.97	75.11	79.76	76.76	79.89
AA (%)	63.90	76.78	83.16	79.60	86.64	86.36	81.12	78.03	88.25	87.64	89.35
κ	0.5395	0.6591	0.6888	0.6642	0.7281	0.7240	0.6852	0.7164	0.7698	0.7382	0.7716

TABLE VI
QUANTITATIVE PERFORMANCE COMPARISON OF DIFFERENT ALGORITHMS IN TERMS OF OA, AA, AND κ ON THE PAVIA UNIVERSITY DATA SET. THE BEST ONE IS SHOWN IN BOLD

Class No.	KNN	RF	SVM	1-D CNN	2-D CNN	3-D CNN	GCN	miniGCN	FuNet-A	FuNet-M	FuNet-C
1	73.86	79.81	74.22	88.90	80.98	80.69	76.49	96.35	96.99	96.47	96.67
2	64.31	54.90	52.79	58.81	81.70	89.12	70.15	89.43	97.74	97.36	97.60
3	55.10	46.34	65.45	73.11	67.99	65.90	62.70	87.01	83.98	83.44	84.49
4	94.95	98.73	97.42	82.07	97.36	98.45	98.35	94.26	96.45	84.40	89.95
5	99.19	99.01	99.46	99.46	99.64	99.19	99.37	99.82	99.55	100.00	99.64
6	65.16	75.94	93.48	97.92	97.59	92.37	83.22	43.12	71.33	85.30	90.56
7	84.30	78.70	87.87	88.07	82.47	76.04	88.38	90.96	66.67	63.80	78.27
8	84.10	90.22	89.39	88.14	97.62	95.81	92.33	77.42	69.61	71.53	71.73
9	98.36	97.99	99.87	99.87	95.60	95.72	95.72	87.27	99.86	99.22	98.04
OA (%)	70.53	69.67	70.82	75.50	86.05	88.44	77.99	89.00	90.34	92.20	
AA (%)	79.68	80.18	84.44	86.26	88.99	88.14	85.19	85.07	86.91	86.84	89.66
κ	0.6268	0.6237	0.6423	0.6948	0.8187	0.8472	0.7196	0.7367	0.8540	0.8709	0.8951

LITERATURE SURVEY - III

Title: FPGA: Fast Patch-Free Global Learning Framework for Fully End-to-End Hyperspectral Image Classification

Author(s): Zhuo Zheng, Student Member, IEEE, Yanfei Zhong, Senior Member, IEEE, Ailong Ma, and Liangpei Zhang, Fellow, IEEE.

Summary of FPGA

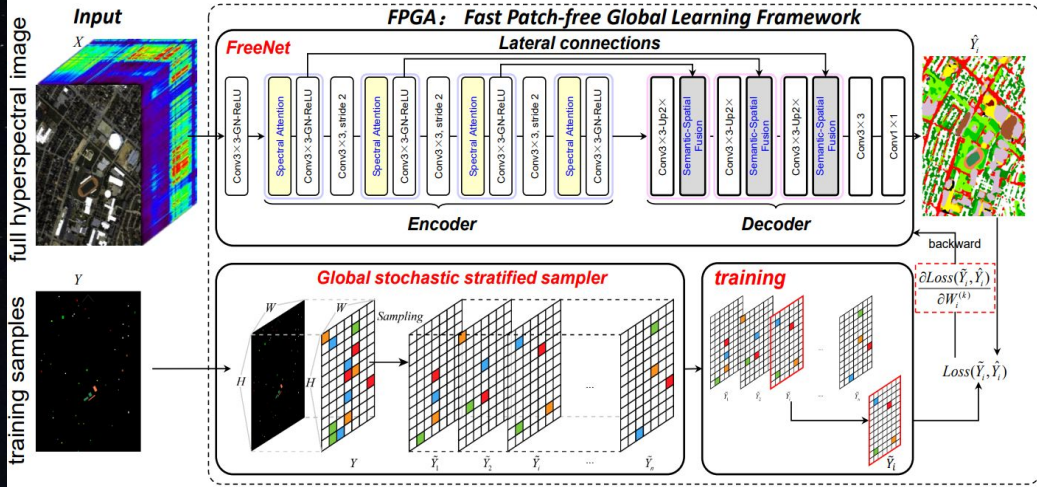
- The FPGA architecture is composed of a **deep convolutional neural network (CNN)** that extracts spectral features from the hyperspectral data and a **global average pooling layer** that aggregates the spectral features into a single feature vector for each pixel.
- Several evaluation metrics are used to measure the accuracy of the model, including overall accuracy, kappa coefficient, and producer's and user's accuracy.
- The drawbacks of the FPGA framework include: the size of the FPGA model can be quite large, which can make it difficult to train and deploy on resource-limited devices; the FPGA model requires a large amount of training data to achieve high accuracy, which can be challenging to obtain for certain applications.

LITERATURE SURVEY - III

Data Set(s)

- ROSIS-03 Pavia University
- Salinas Dataset
- CASI University of Houston

The flow diagram of FPGA model



Result

TABLE II
THE NUMBER OF TRAINING SAMPLES AND TEST SAMPLES FOR THE ROSIS-03 PAVIA UNIVERSITY DATASET

Class	Class name	#Training	#Test	#Total
C1	Asphalt	200	6431	6631
C2	Meadows	200	18449	18649
C3	Gravel	200	1899	2099
C4	Trees	200	2864	3064
C5	Metal Sheets	200	1145	1345
C6	Bare Soil	200	4829	5029
C7	Bitumem	200	1130	1330
C8	Bricks	200	3482	3682
C9	Shadow	200	747	947
Total	-	1800	40976	42776

TABLE III
THE CLASSIFICATION RESULTS OF SVM [8], S-CNN [38], GABOR-CNN [39], DFFN [40], 3D-GAN [51] AND FREE NET ON THE ROSIS-03 PAVIA UNIVERSITY DATASET.

Class	Patch-based					Patch-free
	SVM	S-CNN	Gabor-CNN	DFFN	3D-GAN	FreeNet
C1	85.49	95.47	99.53	99.53	99.18	99.58
C2	92.12	98.71	98.21	97.71	98.86	99.88
C3	85.77	97.32	89.74	99.89	94.94	99.95
C4	96.41	97.72	93.02	97.88	90.15	99.27
C5	98.60	100	99.42	99.48	99.49	100
C6	92.52	97.67	98.77	99.69	98.56	100
C7	93.79	98.36	98.82	100	92.74	100
C8	86.56	95.56	94.12	98.59	97.18	99.83
C9	97.97	100	97.91	99.61	98.51	100
OA(%)	90.78	97.93	97.33	98.57	97.81	99.81
AA(%)	92.14	97.88	96.62	99.16	96.65	99.83
Kappa	0.8813	0.9743	0.9662	0.9808	0.9697	0.9974

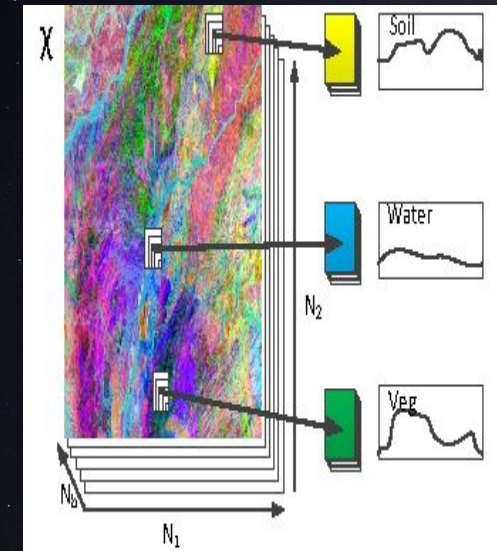
LITERATURE SURVEY - IV

Title: Dual Graph Convolutional Network for Hyperspectral Image Classification With Limited Training Samples

Author(s): Xin He , Yushi Chen ,Member, IEEE, and Pedram Ghamisi ,Senior Member, IEEE

Summary of Dual Graph Convolutional Networks for HIC

- A DGCN, which is a hybrid network of CNN and two graph networks (i.e., the **point graph** and the **distribution graph**), is proposed for HSI classification **with limited training samples**
- Instead of simply applying GCN to classify HSI, the **point graph** aims to fully explore the relationships among samples, and the **distribution graph** utilizes label distribution learning to obtain high correlation features among samples with the same label. The two graphs are integrated with each other to fully extract features among training samples
- In order to mitigate the **overfitting issue** caused by limited HSI training samples, **the drop edge** is investigated in the proposed DGCN
- To further improve the HSI classification results, motivated by the regularization method called **cutout**, we propose a novel technique by improving the cutout with the **multiscale operation to feature maps** in CNN; this method **increases the generalization capability** of the proposed DGCN



LITERATURE SURVEY - IV

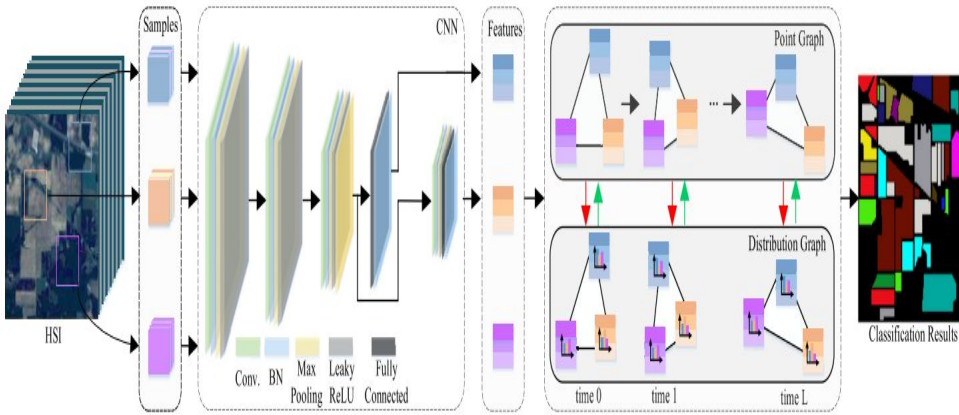
Observation

DGCN for HSI Classification

Data Set(s)

- Indian Pines
- Pavia University
- Houston University
- Salinas Dataset

The flow diagram of SSDGL Framework



Pavia

No.	Class	Name	Sample Number
1		Asphalt	6852
2		Meadows	18686
3		Gravel	2207
4		Trees	3436
5		Metal sheets	1378
6		Bare soil	5104
7		Bitumen	1356
8		Bricks	3878
9		Shadow	1026

CLASSIFICATION RESULTS (VALUES \pm STANDARD DEVIATION) ON THE PAVIA DATA SET USING FIVE TRAINING SAMPLES PER EACH CLASS

Method	EMP-SVM	CNN	EMP-CNN	SCNN	HySN	GCN	DGCN	DGCN-D	DGCN-C	DGCN-M	DGCN-DC
OA(%)	74.71 \pm 3.39	69.42 \pm 2.41	74.01 \pm 4.31	69.01 \pm 6.11	65.76 \pm 4.32	65.12 \pm 2.73	75.60 \pm 6.00	77.21 \pm 4.49	78.28 \pm 3.36	78.40 \pm 4.24	79.87 \pm 5.74
AA(%)	77.22 \pm 2.91	71.91 \pm 2.29	75.75 \pm 4.08	68.89 \pm 5.32	65.99 \pm 3.91	67.51 \pm 1.85	77.05 \pm 5.98	79.80 \pm 4.47	78.46 \pm 3.35	78.43 \pm 4.73	79.84 \pm 5.81
K100	71.45 \pm 3.81	65.47 \pm 2.72	70.67 \pm 5.07	65.21 \pm 8.08	61.26 \pm 4.86	60.56 \pm 3.03	72.75 \pm 6.77	74.26 \pm 5.07	75.46 \pm 3.77	75.61 \pm 4.78	77.09 \pm 6.52
Asphalt	71.87 \pm 10.58	56.50 \pm 5.91	54.38 \pm 9.78	65.94 \pm 5.05	37.43 \pm 20.27	60.15 \pm 13.79	76.10 \pm 5.50	79.45\pm4.22	77.15 \pm 2.87	78.16 \pm 4.04	78.99 \pm 3.62
Meadows	65.36 \pm 21.95	69.71 \pm 12.50	77.65 \pm 12.66	81.62\pm3.23	74.10 \pm 13.18	27.22 \pm 9.14	76.70 \pm 7.11	78.90 \pm 5.05	76.85 \pm 3.89	77.66 \pm 5.18	80.91 \pm 4.72
Gravel	49.25 \pm 11.06	39.51 \pm 10.88	39.88 \pm 23.29	28.98 \pm 12.78	82.86\pm18.29	50.48 \pm 21.65	77.40 \pm 5.91	80.90 \pm 4.45	79.25 \pm 3.96	79.12 \pm 4.63	79.43 \pm 4.02
Trees	89.87\pm10.27	89.61 \pm 5.61	77.76 \pm 16.43	73.26 \pm 5.18	60.18 \pm 18.73	80.35 \pm 10.18	76.50 \pm 5.79	79.60 \pm 4.47	77.85 \pm 2.70	78.15 \pm 4.82	79.23 \pm 4.16
Metal sheets	98.18\pm1.04	90.93 \pm 5.41	92.77 \pm 4.22	75.20 \pm 2.41	94.81 \pm 7.56	96.87 \pm 1.39	78.74 \pm 6.60	80.33 \pm 4.85	77.58 \pm 4.03	78.42 \pm 5.17	80.79 \pm 4.07
Bare soil	77.37 \pm 21.03	58.81 \pm 6.28	79.35 \pm 11.31	73.99 \pm 4.07	71.17 \pm 26.24	96.69\pm29.03	77.35 \pm 5.88	80.15 \pm 4.20	79.65 \pm 3.56	79.11 \pm 4.88	81.03 \pm 3.55
Bitumen	88.82 \pm 6.23	76.61 \pm 9.90	87.16 \pm 4.73	77.86 \pm 8.61	97.57\pm2.85	49.37 \pm 13.71	76.25 \pm 5.94	78.54 \pm 4.67	80.16 \pm 3.59	78.70 \pm 5.12	80.60 \pm 4.41
Bricks	75.26 \pm 12.57	68.78 \pm 8.60	87.46\pm4.81	61.76 \pm 2.45	49.73 \pm 22.57	47.22 \pm 29.92	75.70 \pm 6.20	80.75 \pm 4.72	79.55 \pm 4.32	78.28 \pm 5.18	79.30 \pm 4.16
Shadow	97.73 \pm 1.47	96.72 \pm 1.40	85.33 \pm 9.71	81.37 \pm 7.27	26.10 \pm 14.59	99.22\pm1.01	78.75 \pm 5.46	79.34 \pm 3.86	78.36 \pm 3.12	78.28 \pm 4.35	78.33 \pm 4.83
Training Time (sec.)	4.67	7.13	3.28	357.42	11.33	85.92	260.95	195.20	536.63	388.12	449.25
Test Time (sec.)	0.07	47.74	6.56	883.79	111.53	6.68	164.50	140.91	167.92	125.55	110.42

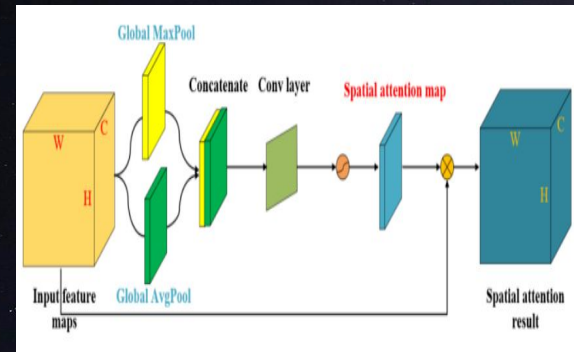
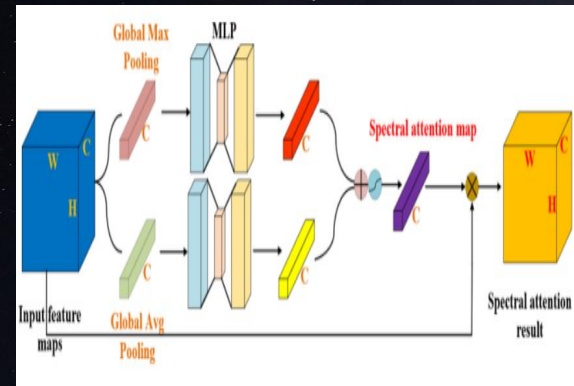
LITERATURE SURVEY - V

Title: A Spectral-Spatial Dependent Global Learning Framework for
Insufficient and Imbalanced Hyperspectral Image Classification

Author(s): Qiqi Zhu, Weihuan Deng, Zhuo Zheng, Yanfei Zhong, Senior
Member, IEEE, Liangpei Zhang, IEEE, Deren Li, IEEE

Summary of Spectral-Spatial Dependent Global Framework

- Spectral-Spatial Dependent Global Learning (SSDGL), combines spectral and spatial information to learn global discriminative features for classification
- The framework includes three modules: a spectral-spatial dependent feature extraction module, a global feature learning module, and a classification module.
- The experimental results show that the SSDGL framework outperforms existing methods in terms of accuracy, especially when dealing with insufficient and imbalanced data



LITERATURE SURVEY - V

Data Set(s)

- Indian Pines Dataset
- Pavia University Dataset
- Houston University Dataset

The flow diagram of SSDGL Framework

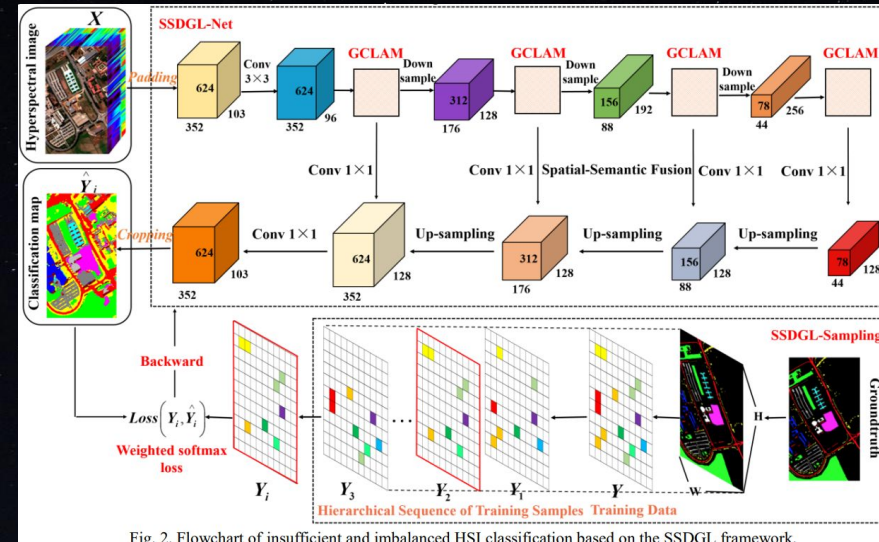


Fig. 2. Flowchart of insufficient and imbalanced HSI classification based on the SSDGL framework.

Observation

THE NUMBER OF TRAINING SAMPLES AND TEST SAMPLES FOR THE INDIAN PINES DATASET

No.	Class.	Train.	Test.	Total.
1	Alfalfa	5	41	46
2	Corn-notill	72	1356	1428
3	Corn-mintill	42	788	830
4	Corn	12	225	237
5	Grass-pasture	25	458	483
6	Grass-trees	37	693	730
7	Grass-pasture-mowed	5	23	28
8	Hay-windrowed	24	454	478
9	Oats	5	15	20
10	Soybean-notill	49	923	972
11	Soybean-mintill	123	2332	2455
12	Soybean-clean	30	563	593
13	Wheat	11	194	205
14	Woods	64	1201	1265
15	Buildings-Grass-Trees	20	366	386
16	Stone-Steel-Towers	5	88	93
Total		529	9720	10249

THE CLASSIFICATION RESULTS OF RBF-SVM, SS-CNN, SSRN, DBMA, MCNN-CONVLSTM, U-NET, FPGA AND SSDGL ON THE INDIAN PINES DATASET WITH 5% LABELED SAMPLES.

Class	CNN-based					FCN-based		
	RBF-SVM	SS-CNN	SSRN	DBMA	MCNN-CONVLSTM	U-Net	FPGA	Proposed
1	70.32	72.14	75.57	90.37	94.36	97.67	97.22	100.00
2	69.63	90.42	90.65	92.72	92.84	92.48	93.07	99.63
3	58.26	81.48	97.01	95.63	93.02	84.77	89.46	99.24
4	45.22	71.23	93.36	89.35	95.32	89.33	100.00	100.00
5	75.48	83.62	98.56	96.92	92.13	81.00	95.63	99.56
6	96.14	97.19	98.94	99.18	98.86	94.08	97.56	100.00
7	95.79	91.03	84.21	79.57	84.83	100.00	100.00	100.00
8	87.72	92.34	98.36	99.11	98.63	98.90	100.00	100.00
9	75.03	96.39	97.61	97.91	92.47	78.95	100.00	100.00
10	66.25	81.75	81.03	92.08	94.76	89.49	96.64	99.68
11	77.62	87.39	93.02	95.15	96.28	97.81	96.74	99.36
12	67.28	83.03	95.72	90.71	94.12	86.50	91.65	99.11
13	96.93	97.42	99.81	99.81	96.95	98.97	100.00	100.00
14	95.07	95.31	95.79	97.11	98.79	98.58	99.91	100.00
15	35.48	74.04	92.25	88.13	92.83	92.08	99.72	100.00
16	97.61	94.61	96.57	97.05	87.32	93.18	100.00	100.00
OA	75.31	89.82	92.21	94.43	94.78	93.20	96.18	99.63
AA	71.12	83.73	93.03	93.81	93.37	92.11	97.33	99.79
Kappa	0.7173	0.8783	0.9115	0.9365	0.9437	0.9222	0.9564	0.9958

IMPLEMENTATION

Before working on the Chandrayaan-2 dataset, we decided to work on Cuprite Dataset which is considered as benchmark for hyperspectral unmixing.

Information about cuprite dataset:-

- No. of bands: 224

Wavelength range: 370-2480nm

No. of end members: Actually 14 but there are minor differences between variants of similar minerals so 12 end members are considered.

Spectral resolution: 10nm

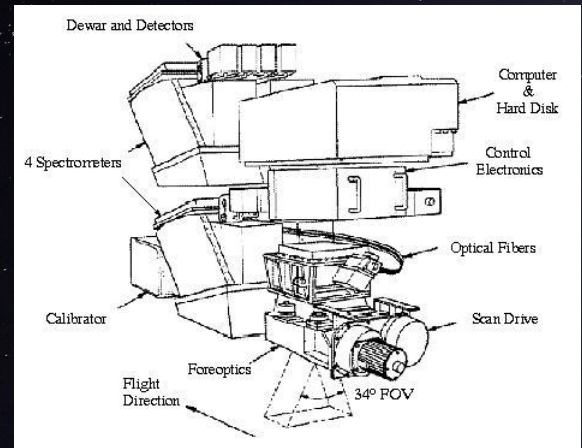
Spatial resolution: 20m

IMPLEMENTATION

Airborne Visible/Infrared Imaging Spectrometer (AVIRIS) sensor was used to capture the cuprite data

Information about AVIRIS sensor:-

- Aircraft used: NASA's ER-2
- Speed of Aircraft: 730 kmph
- Altitude: 20km
- Location: Cuprite mining district, Nevada, U.S

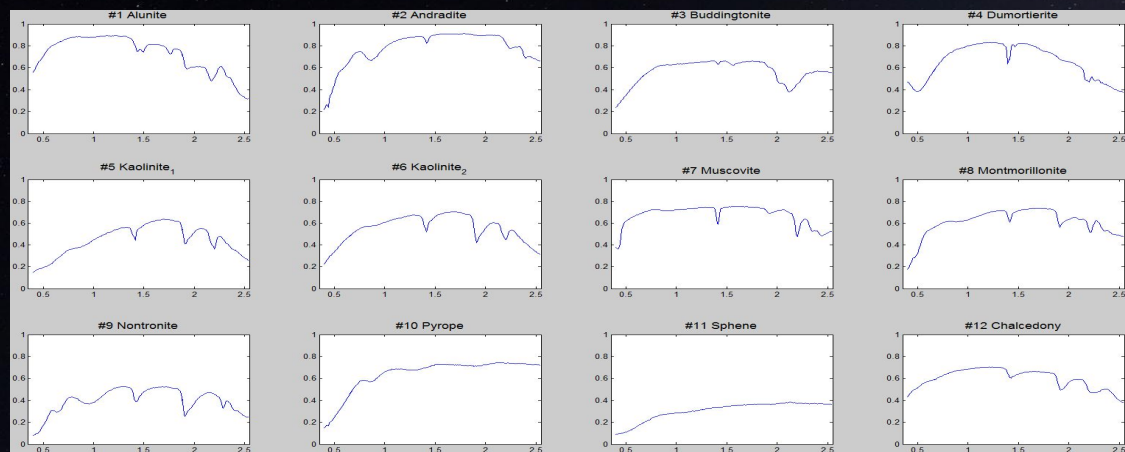


IMPLEMENTATION

Pre-processing of Cuprite Data

As the cuprite dataset is unlabelled, we have pre-processed the data and took few labelled data points using which we can predict the labels of other unlabelled data points with the help of various deep learning models.

Labels of
Cuprite data



IMPLEMENTATION

Implementing 1D-CNN on pre-processed cuprite data

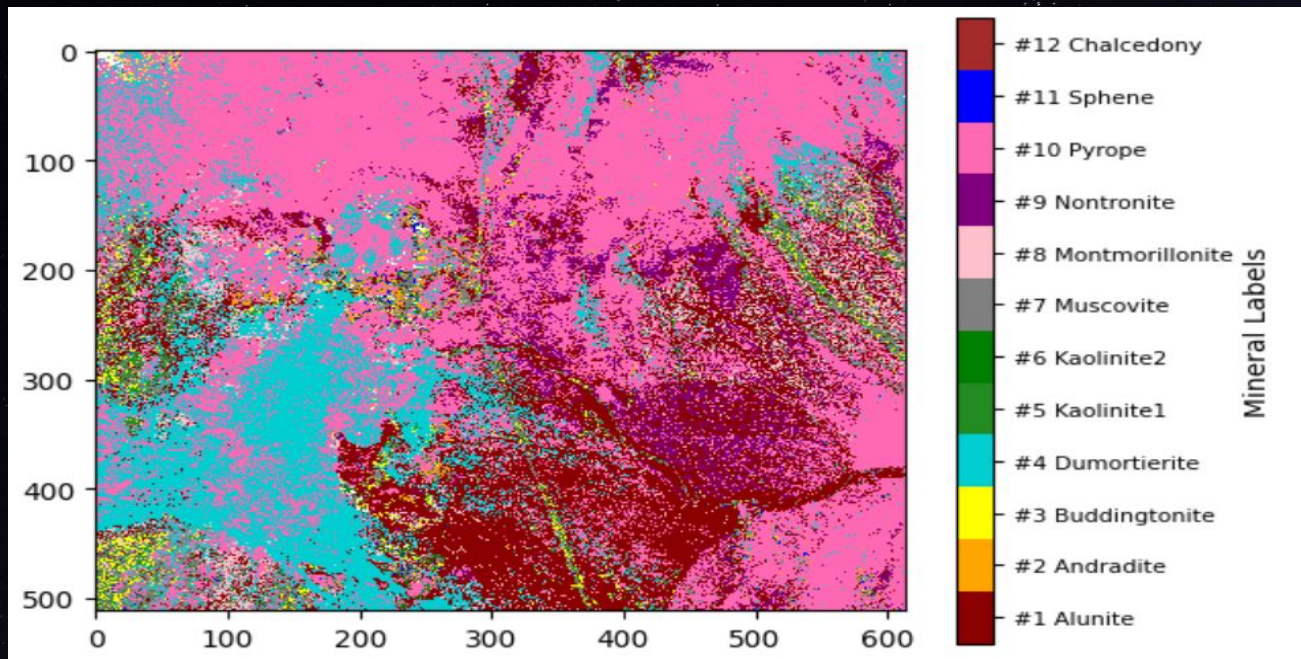
We have implemented 1D CNN on the ~1000 data points extracted during the pre-processing.

Results

```
Confusion Matrix:  
[[16   0   0   0   0   0   1   0   0   0   1   0   0   0]  
[ 0 21   0   0   0   0   0   0   1   0   2   0   0   0]  
[ 0   0  8   0   0   0   2   0   0   0   0   0   0   0]  
[ 0   0   0 13   1   3   0   0   0   0   0   0   0   0]  
[ 0   1   0   0 32   0   0   0   2   0   0   0   0   0]  
[ 0   0   0   0   0 11   0   0   3   0   0   0   0   0]  
[ 1   0   0   1   0   0   9   2   0   0   0   0   0   0]  
[ 0   3   1   1   0   1   1 18   0   0   0   0   0   1]  
[ 0   1   0   0   0   0   0   0   0 58   0   0   0   0]  
[ 0   0   0   0   0   0   0   0   0   0 45   0   0   0]  
[ 0   0   0   0   0   0   0   0   0   6 37   0   0   0]  
[ 0   0   0   1   0   1   2   1   0   0   0   0   0   6]]  
Accuracy: 0.8698412698412699  
Precision: 0.845041823529268  
Recall: 0.816848388754038  
F1-score: 0.8254094805359907  
ROC AUC score: 0.977411523233787
```

IMPLEMENTATION

Predicted labels of Cuprite data by 1D CNN:



IMPLEMENTATION

Implementing 2D-CNN on pre-processed cuprite data

We have implemented 2D CNN on the ~1000 data points extracted during the pre-processing.

Results

Confusion Matrix:

```
[[16  0  0  0  0  2  0  0  0  0  0  0  0]
 [ 0 21  0  0  0  0  0  1  0  1  1  1  0]
 [ 0  1  6  0  0  0  2  1  0  0  0  0  0]
 [ 0  0  0 11  0  5  0  1  0  0  0  0  0]
 [ 0  0  0  0 33  0  0  0  2  0  0  0  0]
 [ 0  0  0  0  0 12  0  0  2  0  0  0  0]
 [ 1  0  0  0  0  0  8  3  0  0  0  0  1]
 [ 0  0  0  1  0  1  0 24  0  0  0  0  0]
 [ 0  0  0  0  0  0  0  1 58  0  0  0  0]
 [ 0  0  0  0  0  0  0  0  0 43  2  0  0]
 [ 0  0  0  0  0  0  0  0  0  1 42  0  0]
 [ 0  0  0  0  0  1  0  0  1  0  0  0  0]]
```

Accuracy: 0.8984126984126984

Precision: 0.8889612100949863

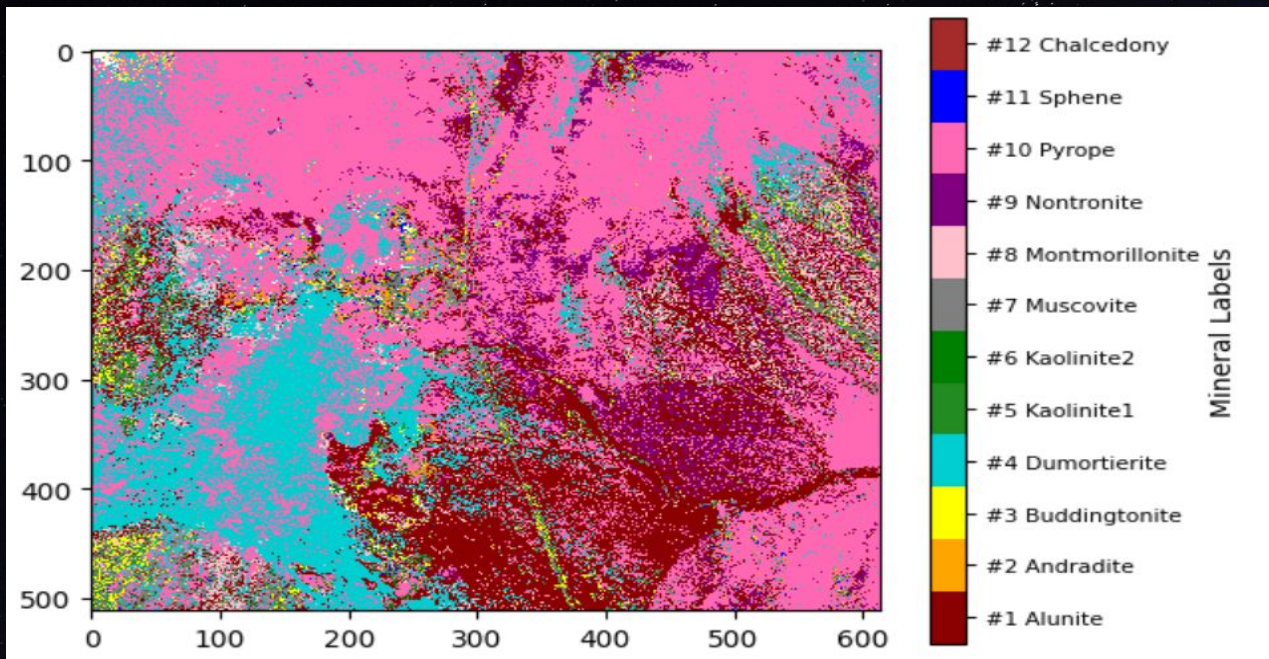
Recall: 0.8402451381767793

F1-score: 0.8540061149713427

ROC AUC score: 0.9868236470641417

IMPLEMENTATION

Predicted labels of Cuprite data by 2D CNN:



IMPLEMENTATION

Implementing HybridSN on Indian Pines Dataset

We have implemented HybridSN on the Indian Pines dataset.

Results

- | |
|--|
| 8.0268032848835 Test loss (%) |
| 97.40766286849976 Test accuracy (%) |
| 97.04344405901733 Kappa accuracy (%) |
| 97.40766550522648 Overall accuracy (%) |
| 91.50028672147462 Average accuracy (%) |

IMPLEMENTATION

Implementing HybridSN on pre-processed cuprite data

We have implemented 2D CNN on the ~4812 data points extracted during the pre-processing.

- Results

- Train Accuracy:

```
52/52 [=====] - 75s 1s/step - loss: 0.1237 - accuracy: 0.9575
```

- Test Report (for Alunite):

```
precision: 86.77685950413223%
recall: 87.5%
f1-score: 87.136929460580912%
```

07

TIMELINE

CONCLUSION

Why only CNN ?

- Compare to other methods like GCN the computational complexity of CNN is less
- The Convolution filter can capture can capture high dimensional image data in an effective way without loss of information

1D CNN vs 2D CNN vs 3D CNN

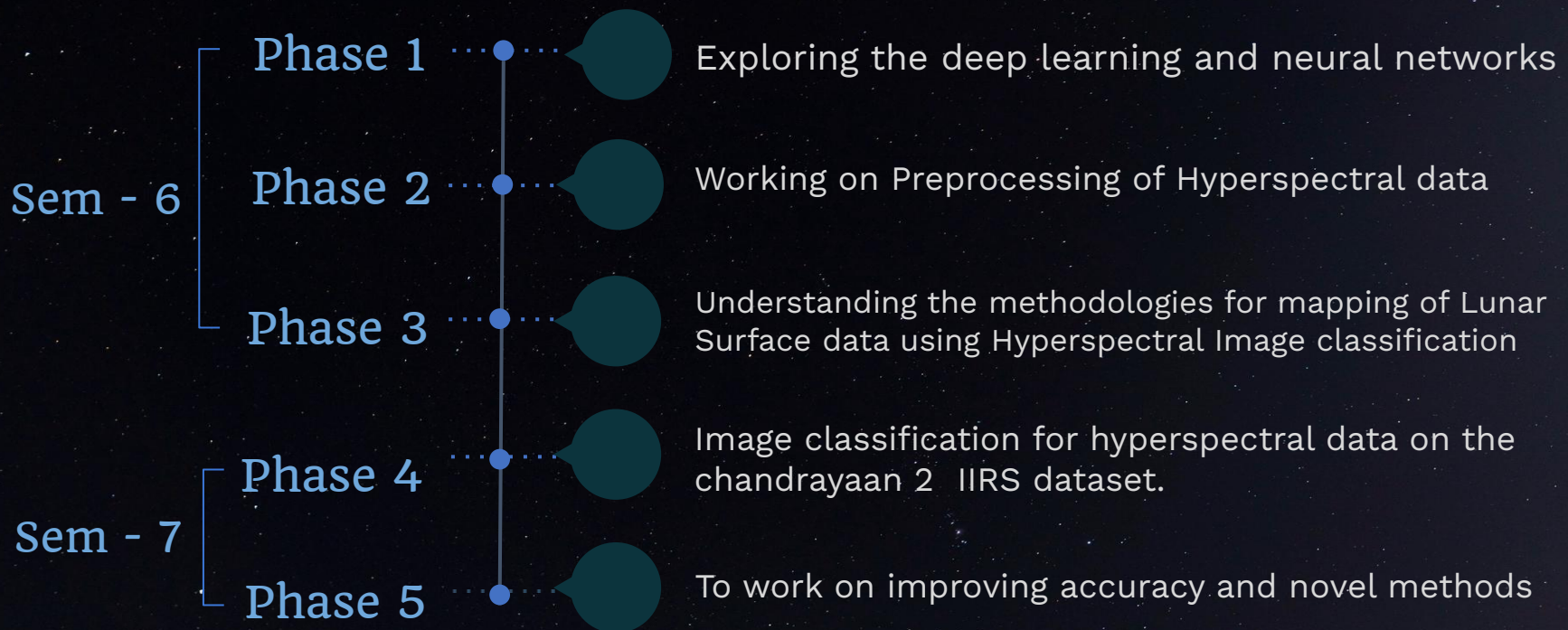
- 1D CNN captures only spectral data
- 2D CNN captures only spatial data
- 3D CNN captures both spatial and spectral data but computational cost is high when compared to 1D and 2D CNN
- HybridSN just like 3D CNN captures both spatial and spectral data but computational cost is less compared to 3D CNN

CURRENT AND FUTURE WORK

Implementing HybridSN on Cuprite Data set:

- We are currently working on HybridSN implementation on cuprite dataset (Benchmark). As of today (05-06-2023) we have got the classification report of one label out of twelve labels. Within 7-10 days we will get the classification report of all the labels.
- If we are able to get the high overall accuracy then we implement it on IIRIS Data Set.
- If possible we will try to propose our own novel method.

TIMELINE



REFERENCES

- “Dual Graph Convolutional Network for Hyperspectral Image Classification With Limited Training Samples” by Xin He , Yushi Chen ,and Pedram Ghamisi. (2021)
- A Spectral-Spatial Dependent Global Learning Framework for Insufficient and Imbalance Hyperspectral Image Classification by Qiqi Zhu, Weihuan Deng, Zuo Zheng, Yanfei Zhong. (2021)
- “HybridSN: Exploring 3D-2D CNN Feature Hierarchy for Hyperspectral Image Classification” by Li et al. (2021)
- “Graph Convolutional Networks for Hyperspectral Image Classification” Danfeng Hong , Member, IEEE, Lianru Gao , Senior Member, IEEE. (2020)
- “FPGA: Fast Patch-Free Global Learning Framework for Fully End-to-End Hyperspectral Image Classification” by Zhang et al. (2021)

A large, abstract graphic on the left side of the slide consists of several concentric circles and arcs. The outermost circle is filled with vertical cyan lines. Inside it is a cyan dotted circle, followed by a cyan solid circle, and a purple dashed circle. The innermost circle is a cyan solid circle. The entire graphic is set against a dark background.

Thank You